Thermochimica Acta 498 (2010) 92–99

Contents lists available at ScienceDirect

Thermochimica Acta

journal homepage: www.elsevier.com/locate/tca

Flame retardancy mechanisms of bisphenol A bis(diphenyl phosphate) in combination with zinc borate in bisphenol A polycarbonate/acrylonitrile–butadiene–styrene blends

Kristin H. Pawlowski[a], Bernhard Schartel[a,*], Mario A. Fichera[b], Christian Jäger[b]

[a] BAM Federal Institute for Material Research and Testing, Unter den Eichen 87, 12205 Berlin, Germany
[b] BAM Federal Institute for Material Research and Testing, Richard-Willstaetter Str. 11, 12489 Berlin, Germany

ARTICLE INFO

Article history:
Received 13 July 2009
Received in revised form
10 September 2009
Accepted 8 October 2009
Available online 7 November 2009

Keywords:
Flame retardancy
PC/ABS
Aryl phosphate
Zinc borate
Flammability

ABSTRACT

Bisphenol A polycarbonate/acrylonitrile–butadiene–styrene (PC/ABS) with and without bisphenol A bis(diphenyl phosphate) (BDP) and 5 wt.% zinc borate (Znb) were investigated. The pyrolysis was studied by thermogravimetry (TG), TG-FTIR and NMR, the fire behaviour with a cone calorimeter applying different heat fluxes, LOI and UL 94. Fire residues were examined with NMR.

BDP affects the decomposition of PC/ABS and acts as a flame retardant in the gas and condensed phases. The addition of Znb results in an additional hydrolysis of PC. The fire behaviour is similar to PC/ABS, aside from a slightly increased LOI and a reduced peak heat release rate, both caused by borates improving the barrier properties of the char. In PC/ABS + BDP + Znb, the addition of Znb yields a borate network and amorphous phosphates. Znb also reacts with BDP to form alpha-zinc phosphate and borophosphates that suppress the original flame retardancy mechanisms of BDP. The inorganic–organic residue formed provides more effective flame retardancy, in particular at low irradiation in the cone calorimeter, and a clear synergy in LOI, whereas for more developed fires BDP + Znb become less effective than BDP in PC/ABS with respect to the total heat evolved.

1. Introduction

Bisphenol A polycarbonate/acrylonitrile–butadiene–styrene polymer blends (PC/ABS) are used in engineering for electronic devices and applications like transportation, which have high demands on fire behaviour. Within all flame retardants used in PC/ABS, aryl phosphates, including bisphenol A bis(diphenyl phosphate) (BDP) and resorcinol bis(diphenyl phosphate) (RDP), are successful alternatives for flame retardants containing halogen. They are the most commonly used halogen-free flame retardants in PC/ABS [1–3].

The flame retardancy mechanisms of aryl phosphates in PC/ABS were examined by Levchik et al. [4,5]. In an earlier paper we discussed the detailed thermal decomposition and fire behaviour of BDP in PC/ABS [6]. BDP acts in both the condensed and gas phases. Charring is caused by induced cross-linking, whereby BDP acts like an acid precursor, and by the active incorporation of phosphate groups into the network. In the gas phase, BDP acts by flame inhibition, probably by providing volatile PO, P and P_2 species [7–9].

To satisfy the increasing demands on flame retardancy efficiency and combinations of properties, approaches have been made to combine different flame retardants or flame retardants with adjuvants, respectively, and thus to obtain new, superior synergisms [10–13]. The combination of BDP with nano-dispersed boehmite, as reported in an earlier study [14], yielded a synergism with regard to LOI but showed antagonism in the charring of PC and BDP.

PC/ABS blends usually show relatively high smoke release. Flame inhibition increases smoke release because of incomplete oxidation. Zinc borate (Znb) is known as a multifunctional polymer additive [15]. It is applied as a flame retardant, afterglow suppressant, anti-tracking agent and is often used as smoke suppressant, e.g. in PVC [16]. In general, smoke suppression is believed to be achieved through different mechanisms in the condensed phase or the gas phase, such as the elimination of carbon black precursors or the removal of nucleation germs. Further, Znb is already used as a flame retardant in pure PC, resulting in a significant increase in LOI [17].

Hence in this study, the flame retardancy effect of BDP with 5 wt.% Znb in PC/ABS and PC/ABS with 5 wt.% Znb is studied. The focus was on the interaction of BDP with Znb and on its influence on the flame retardancy mechanisms, to reveal synergisms or antagonisms. Therefore this contribution lays important groundwork to refine the halogen-free fire retardancy of PC/ABS.

* Corresponding author. Tel.: +49 30 8104 1021; fax: +49 30 8104 1617.
E-mail address: bernhard.schartel@bam.de (B. Schartel).

0040-6031/$ – see front matter © 2009 Elsevier B.V. All rights reserved.
doi:10.1016/j.tca.2009.10.007

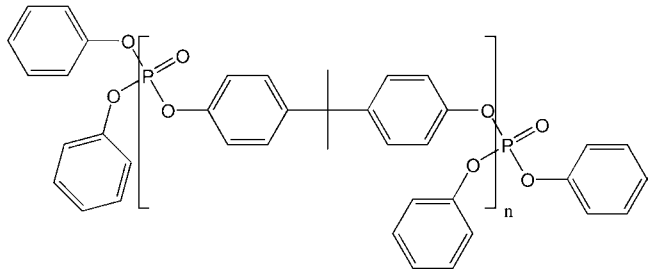

Fig. 1. Structure of BDP.

2. Experimental

Four different PC/ABS blends were investigated: PC/ABS with and without BDP, with 5 wt.% Znb and with BDP and 5 wt.% Znb. A PC:ABS ratio of 4.7:1 was maintained at all times. The A:B:S ratio of ABS was 21:13:66. In all systems a master batch was added, consisting of polytetrafluoroethylene (PTFE) and SAN in the ratio 1:1. The molecular weight of BDP (Fig. 1) with $n = 1$ is $M_{wBDP(n=1)} = 692.6\,g\,mol^{-1}$. The oligomeric BDP used had an averaged repeating unit of $n = 1.1$ and contained about 2.5 wt.% TPP (triphenyl phosphate). Znb had the molecular formula $2(ZnO)3(B_2O_3)3.5(H_2O)$ and a molecular weight of $434.7\,g\,mol^{-1}$. The samples were provided by Bayer MaterialScience AG (Dormagen, Germany) and their contents are shown in Table 1.

Thermal decomposition was investigated by thermogravimetry (TG) (TGA/SDTA 851, Mettler Toledo, Germany). For evolved gas analysis, the same TG coupled with a Fourier transform infrared spectrometer (TG-FTIR, Nexus 470, Nicolet, Germany) was used. All measurements were performed under nitrogen with a heating rate of $10\,K\,min^{-1}$ and a sample weight of 10 mg. Decomposition kinetics were based on varying heating rates (2, 5 and $10\,K\,min^{-1}$). Values for residue were taken at the end of the main decomposition step. The standard deviation for TGA was about 1 wt.%, which included the contribution of buoyant forces.

To analyse the forced-flaming behaviour [18], a cone calorimeter from FTT, UK was used, according to ISO 5660. The samples (100 mm × 100 mm × 3 mm) were measured horizontally in a frame, using different external heat fluxes (35, 50 and $70\,kW\,m^{-2}$). The total heat release (THR) was taken at the time of flame-out. The flammability was determined by the UL 94 test according to IEC60695-11-10 (sample size: 120 mm × 12.5 mm × 3 mm × 1.5 mm) and by limiting oxygen test (LOI), following ISO 4589 (sample size: 80 mm × 10 mm × 4 mm).

Solid-state nuclear magnetic resonance (NMR) was used to analyse the residues of heat-treated samples and cone calorimeter measurements. The thermal treatment was carried out in a horizontal quartz tube furnace under air and nitrogen flow ($200\,ml\,min^{-1}$), in a temperature range between 610 and 820 K. The samples were heated at a heating rate of $10\,K\,min^{-1}$, holding the final temperatures for 10 min before cooling down again. To obtain residues from cone calorimeter measurements, samples were burned for 65 and 147 s, respectively, and quenched in liquid nitrogen to ensure rapid cooling and avoid oxidation. The NMR measurements were performed using an AVANCE 600 and a DMX 400 spectrometer (Bruker Biospin GmbH, Rheinstetten, Germany). Magic angle sample spinning (MAS) was applied using 4 mm zirconia rotors. All MAS experiments were carried out at room temperature. ^{13}C NMR spectra were recorded at a Larmor frequency of 100.6 MHz with a 4 mm double-resonance probe. Due to the low natural abundance of ^{13}C (1.1%), cross-polarisation with magic angle sample spinning (CPMAS) was used. The ^{1}H 90° pulse length was 2.8 μs, a CP contact time of 0.5–4.0 ms was used with repetition times of 3 s. The carbon spin-lock field strength was held constant, while the proton spin-lock field was ramped down to 50% of the initial value during CP. Proton decoupling was carried out with a 15° two-pulse phase modulation (TPPM) sequence. ^{13}C chemical shifts were referenced using the glycine **C**OOH signal set to $\delta(^{13}C) = 176.4$ ppm as a secondary standard. The MAS frequency was 13 kHz. ^{31}P NMR spectra were acquired at a Larmor frequency of 161.9 MHz (DMX 400) with a 4 mm double-resonance MAS NMR probe, a spinning speed of 13 kHz and single-pulse excitation with a 90°-pulse length of 5.5 μs. To ensure full relaxation a repetition time of 600 s was used. The ^{31}P chemical shifts were referenced to 85% phosphoric acid at $\delta(^{31}P) = 0$ ppm via the secondary standard hydroxyapatite at $\delta(^{31}P) = 2.3$ ppm. ^{11}B NMR was carried out at 192.5 MHz (Avance 600) with single-pulse excitation using a selective 90° pulse of 1.25 μs, a MAS frequency of 10 kHz and a relaxation delay of 10 s. Chemical shifts are reported relative to $BF_3(OEt_2)$ using the narrow signal of crystalline BPO_4 at $\delta(^{11}B) = -4.1$ ppm as an external secondary standard.

Table 1
Investigated materials (remaining wt.% other additives).

PC/ABS + . . .	/	BDP	5 wt.% Znb	BDP + 5 wt.% Znb
PC	81.2	71.0	77.1	66.8
ABS	17.3	15.0	16.4	14.2
PTFE/SAN	0.9	0.9	0.9	0.9
BDP		12.5		12.5
Znb			5.0	5.0

3. Results and discussion

3.1. Thermal decomposition

The TG results of PC/ABS, PC/ABS + BDP, PC/ABS + 5 wt.% Znb and PC/ABS + BDP + 5 wt.% Znb are summarized in Table 2 and the corresponding masses and mass loss rates are shown in Fig. 2. PC/ABS, PC/ABS + BDP, PC/ABS + 5 wt.% Znb and PC/ABS + BDP + 5 wt.% Znb all decomposed in two main decomposition steps. The decomposition of PC/ABS and PC/ABS + BDP was discussed in detail in a previous paper [6]. As main results the first decomposition step was related to the ABS decomposition and the second to PC, which was confirmed by the characteristic decomposition temperatures, the mass losses (both Fig. 2 and Table 2) and volatile pyrolysis products (Fig. 3). The addition of BDP to PC/ABS led to a shift in the temperature (+24 K) of the maximum weight loss of PC to higher temperatures. Further, there was a decrease in the decomposition temperature of ABS. The shifting of the decomposition temperature of PC to higher and of ABS to lower temperatures resulted in a clear separation of both decomposition steps, as seen in Fig. 2. The residue increased further when BDP was added. This increase in char resulted from an interaction of BDP with PC. BDP acts hereby as an acid precursor which induces the charring and performs cross-linking with decomposition products of PC, probably

Table 2
Thermal analysis of PC/ABS, PC/ABS + BDP, PC/ABS + Znb and PC/ABS + BDP + Znb under nitrogen at a heating rate of $10\,K\,min^{-1}$.

PC/ABS + . . .	/	BDP	5 wt.% Znb	BDP + 5 wt.% Znb	Error
T_{onset} in K	681	673	682	669	±2
Mass loss I (decomposition of ABS)					
Weight loss in wt.%	20.9	24.7	29.5	25.9	±1
T_{max1} in K	715	699	711	706	±2
Mass loss II (decomposition of PC)					
Weight loss in wt.%	56.4	46.6	43.9	43.4	±1
T_{max2} in K	776	800	778	798	±2
Residue					
Mass in wt.%	22.7	28.7	26.6	30.7	±1

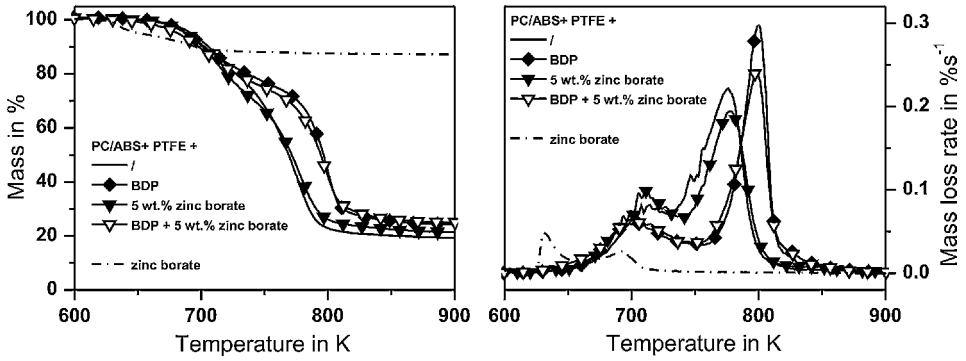

Fig. 2. Mass loss and mass loss rates of PC/ABS, PC/ABS + BDP, PC/ABS + Znb and PC/ABS + BDP + Znb and Znb alone, measured with TG in nitrogen atmosphere at a heating rate of 10 K min^{-1}.

with phenolic groups of PC generated through Fries rearrangement.

The decomposition of Znb resulted in a significant release of water (around 13 wt.%). However PC/ABS + Znb did not show an additional third decomposition step due to the partial hydrolysis of PC, as was reported for PC/ABS + boehmite [14]. Adding 5 wt.% of Znb to PC/ABS resulted in an onset temperature (T_{onset}) identical to the one for PC/ABS, and in very similar temperatures for the maximum weight loss rate (T_{max}) in both the first decomposition step and the PC-related second decomposition step (Table 2). Therefore, at first glance adding Znb and thus releasing water had no influence on the decomposition temperatures of the polymer, whereas the mass losses of the two decomposition steps in PC/ABS + Znb differed significantly from the ones of PC/ABS. For the first decomposition step there was an increase of 8.6 wt.% compared to PC/ABS. The resulting value can not be explained only by the pyrolysis of ABS and Znb water release (25.9 wt.% > 16 + 0.6 wt.%). The mass loss during the second decomposition step decreases correspondingly by 12.5 wt.%. Thus PC hydrolyses partially at lower temperatures, coinciding with the decomposition of ABS. This conclusion was confirmed by the earlier beginning of product release rates of CO_2 and phenol derivatives (Fig. 3).

The residue of PC/ABS + Znb was very similar to that calculated for a superposition of the effects of PC/ABS and Znb, when they decompose separately (26.6 wt.% ≈ 21.5 + 4.5 wt.%). This is somehow surprising, considering the additional hydrolysis of PC.

For PC/ABS + BDP + Znb the mass loss of the first decomposition step was increased only slightly (1.2 wt.%) compared to PC/ABS + BDP without Znb (Table 2). The mass loss of the second PC decomposition step was also quite similar to the one for PC/ABS + BDP, considering that for PC/ABS + BDP + Znb less polymer decomposes than in PC/ABS + BDP. It is assumed that BDP reacts instead of PC with some of the water released by Znb. Further the decomposition temperatures were quite similar for PC/ABS + BDP with and without Znb. PC/ABS + BDP + Znb had an onset temperature, temperature of the maximum mass loss rate for the first decomposition step, and temperature of the maximum mass loss rate for the second decomposition step that differed by only 2–7 K from those of PC/ABS + BDP (Table 2). The residue was a little bit less than that calculated taking into consideration that PC/ABS + BDP and Znb decomposed separately (30.7 wt.% < 31.7 wt.%). Comparing the data observed for PC/ABS + BDP + Znb with those for PC/ABS + Znb and PC/ABS + BDP, a significant interaction between BDP and Znb became obvious. Most probably alternative reactions occurred to the reaction of BDP with PC and the water release of Znb and PC.

The product release rates also showed this effect of adding Znb in PC/ABS + BDP + Znb (Fig. 3). As shown in an earlier paper [6], adding BDP in PC/ABS + BDP results in an increase of CO_2 and a decrease in phenol release. It was concluded that the enhanced charring of PC/ABS + BDP was accompanied by this change in volatile release rates. For PC/ABS + BDP + Znb there was less CO_2 production than for PC/ABS + BDP. Further for PC/ABS + BDP + Znb there was an increased release of phenol derivatives. Actually both the CO_2 and the phenol release of PC/ABS, PC/ABS + Znb and PC/ABS + BDP + Znb were quite similar, whereas only PC/ABS + BDP showed a clearly different behaviour.

The reaction kinetics in Fig. 4 shows at least two main activation energies for PC/ABS, the first at around 180 kJ mol^{-1} and the second at around 230 kJ mol^{-1}. These values were related to the decomposition dominated by ABS and PC, respectively. The decomposition of ABS and PC overlapped strongly for PC/ABS, which is shown clearly by decreasing and increasing activation energies rather than constant plateau values. Between the conversion regions related to ABS and PC decomposition, respectively, a clear minimum in activation energy occurs between 15% and 40% of conversion, indi-

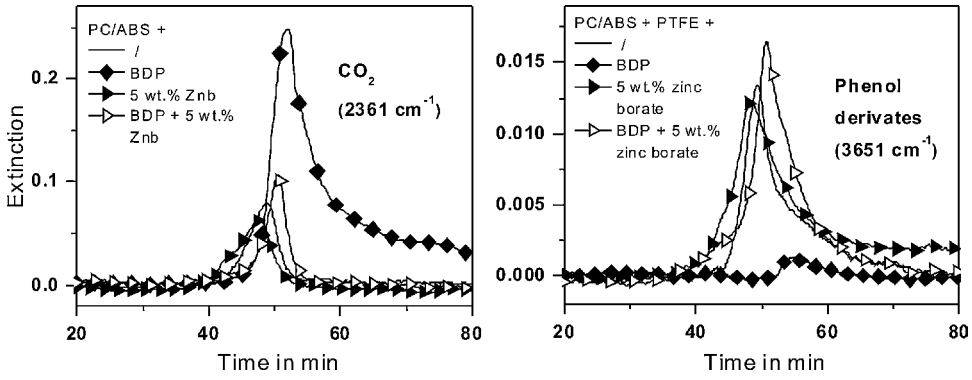

Fig. 3. Pyrolysis product release rates determined by TG-FTIR for CO_2 and phenol derivatives, comparing PC/ABS, PC/ABS + BDP, PC/ABS + Znb and PC/ABS + BDP + Znb.

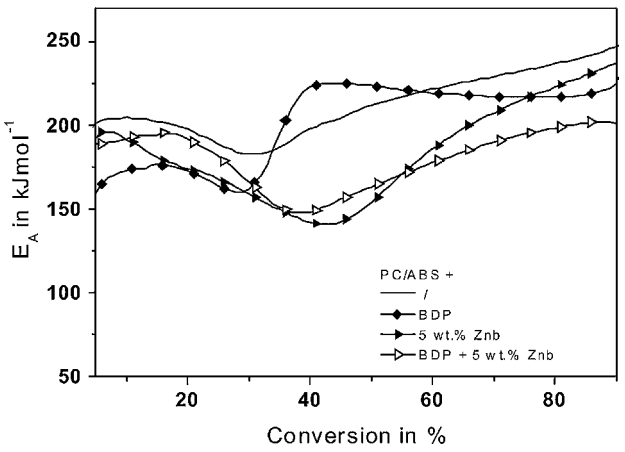

Fig. 4. Activation energy (E_A) versus conversion, comparing PC/ABS, PC/ABS + BDP, PC/ABS + Znb and PC/ABS + BDP + Znb.

cating the interaction between the two decomposition processes. Adding BDP to PC/ABS results in separation of the decomposition processes. Consequently two plateau activation energies were observed. The first plateau at about 170 kJ mol^{-1} corresponded to the ABS decomposition. The second plateau at 220 kJ mol^{-1} represented the PC decomposition. They are separated by a minimum in activation energy at between 23% and 33% conversion, indicating the reduced interaction between ABS decomposition products and PC decomposition during the beginning of PC decomposition. For PC/ABS + Znb and PC/ABS + BDP + Znb, clearly stronger minima were observed between 25 and 50% of conversion. This indicates the partial hydrolysis of PC. Further the activation energy was increased for ABS and decreased for PC in the samples containing Znb.

^{13}C solid-state NMR investigations of the residue were performed to examine the decomposition of PC in PC/ABS + Znb and PC/ABS + BDP + Znb. Fig. 5 shows the spectra for the PC/ABS + Znb system on the left and for PC/ABS + BDP + Znb on the right, for sample heat treatments at 670, 730 and 820 K. The peak assignment for the PC signals is also shown on the left. It should be noted that the BDP ^{13}C solid-state NMR signals cannot be distinguished from the PC ones, such that no further assignment is given on the right. The main results can be summarized as follows: (i) the signals at 150 ppm was higher for the system with BDP than for PC/ABS + Znb without BDP; (ii) with BDP the PC matrix decomposes at higher temperatures (best seen by a comparison of the spectra taken after 730 K heat treatment), resulting in an NMR spectrum typical for aromatic, sp^2-hybridized C-atoms [19] and thus for char; and (iii) a new signal at about 140 ppm emerges particularly in the PC/ABS + BDP + Znb system (assigned by C_8).

Note that the temperature program for preparing the solid residues investigated by NMR was different from the constant heating rate used in TG. Taking into account that the same mass loss is observed 50 K earlier, the results correspond with the results of thermal analysis, both showing an increase in the thermal stability of PC by BDP. The new peak at 140 ppm can be assigned to xanthon-like structures. In the literature [1,20] xanthons already have been described for the decomposition of PC, as secondary products which result from such phenomena as Fries rearrangements (Fig. 6). This signal was more pronounced for PC/ABS + BDP + Znb than for PC/ABS + Znb. The reason for this is the acidic character of BDP at high temperatures which supports Fries rearrangements, resulting in more xanthon-like structures in the char.

The ^{31}P NMR spectra of the solid residues of PC/ABS + BDP + Znb samples as a function of the temperature are shown in the left of Fig. 7. The spectrum at 670 K is the same as for non-heat-treated samples. There is a broad peak at −19.2 ppm (signal width = 1100 Hz) indicating the BDP structure in the solid state. ^{31}P NMR investigation of the liquid BDP showed a corresponding sharp peak at −17.6 ppm with a signal width of 144 Hz. The difference in state of aggregation is due to the molecular mixing of BDP in PC/ABS. The signal of BDP decrease due to the release of phosphate into the gas phase, the reaction of BDP with zinc borate and the formation of different kind of phosphates in the condensed phase: crystalline and amorphous orthophosphates (PO_4), O_3P–O–PO_3, O_3P–O–PO_2–O–PO_3, O_3P–O–PO_2–O–PO_2–O–PO_3, up to polyphosphates. The ratio between P and O is 1:4 for orthophosphates and approaches 1:2 for polyphosphates. First decomposition products occurred at >760 K, where a broad signal around 0 ppm emerges. At higher temperatures α-$Zn_3(PO_4)_2$ and BPO_4 are formed as a result of a reaction between BDP as the only phosphate-containing phase and Znb. However, the main phosphate part in the solid residues forms amorphous structures as seen by the broad peak pattern ranging from about 20 to −20 ppm.

The ^{11}B NMR spectra as function of the temperature are shown in the right of Fig. 7. All spectra show the presence of planar BO_3 units (20–7 ppm region, typical second-order quadrupolar peak shape) and tetragonal BO_4 groups (narrow peak at 0 ppm). The main results are that with increasing temperature (i) the BO_3/BO_4 ratio rises, (ii) an amorphous borate network forms which contains the main borate content, and (iii) for temperatures higher than 790 K BPO_4 (signal at around −5 ppm) [21] occurs. The change in BO_3/BO_4 ratio and the formation of an amorphous borate network is analogous to the changes observed for the phosphates in the ^{31}P NMR. The BPO_4 formation was consistently observed by both the ^{11}B NMR and the ^{31}P NMR investigation.

Based on the changes in the products released and the pyrolysis products observed in the solid state in particular, we concluded that the reaction between BDP and Znb reduces the amount of phosphorus performing cross-linking. Further the temperature > 760–790 K observed for the reaction between BDP and Znb corresponds to a mass loss > 55 wt.%. This indicates that in the beginning of PC decomposition BDP is still available to perform cross-linking with PC in PC/ABS + BDP + Znb, similar to PC/ABS + BDP. This interpretation corresponds to the shift in PC decomposition temperature in PC/ABS + BDP + Znb, similar to PC/ABS + BDP. Only at higher temperatures the cross-linking mechanism was eliminated between BDP and PC decomposition products.

3.2. Fire behaviour

The results for time to ignition (t_{ign}, cone calorimeter with an irradiation of 35 kW m^{-2}), for flammability (reaction to small flame: LOI and UL 94) and for forced-flaming fire behaviour (cone calorimeter with three different heat fluxes) are summarized in Table 3 and illustrated in Fig. 8. The t_{ign} was increased significantly by adding BDP to PC/ABS (+13 s). The addition of 5 wt.% Znb to PC/ABS led to a decreased t_{ign} (−8 s). Also the combination of BDP and Znb resulted in a worsened t_{ign} (−7 s) for PC/ABS + BDP + Znb. For the flammability, PC/ABS combined with BDP resulted in an increase in LOI from 23.6% to 28.1% (+4.5%). The addition of 5 wt.% Znb to PC/ABS provided for some minor improvement in the LOI (+1.9%). The best result was achieved for the combination of BDP and Znb, with a LOI of 32.7%, revealing a clear synergistic effect in LOI (+9.1% > +(4.5% + 1.9%)).

PC/ABS and PC/ABS + Znb achieved HB classification in the UL 94. Adding BDP to PC/ABS yielded V-0 for both 1.5 and 3 mm thick samples, with almost immediate self-extinction after removing the burner. PC/ABS + BDP + Znb showed V-0 for the 3 mm thick samples and V-1 for the 1.5 mm thick specimens, because of burning slightly longer than 10 s. Thus combining BDP and Znb revealed a slight antagonism with respect to UL 94.

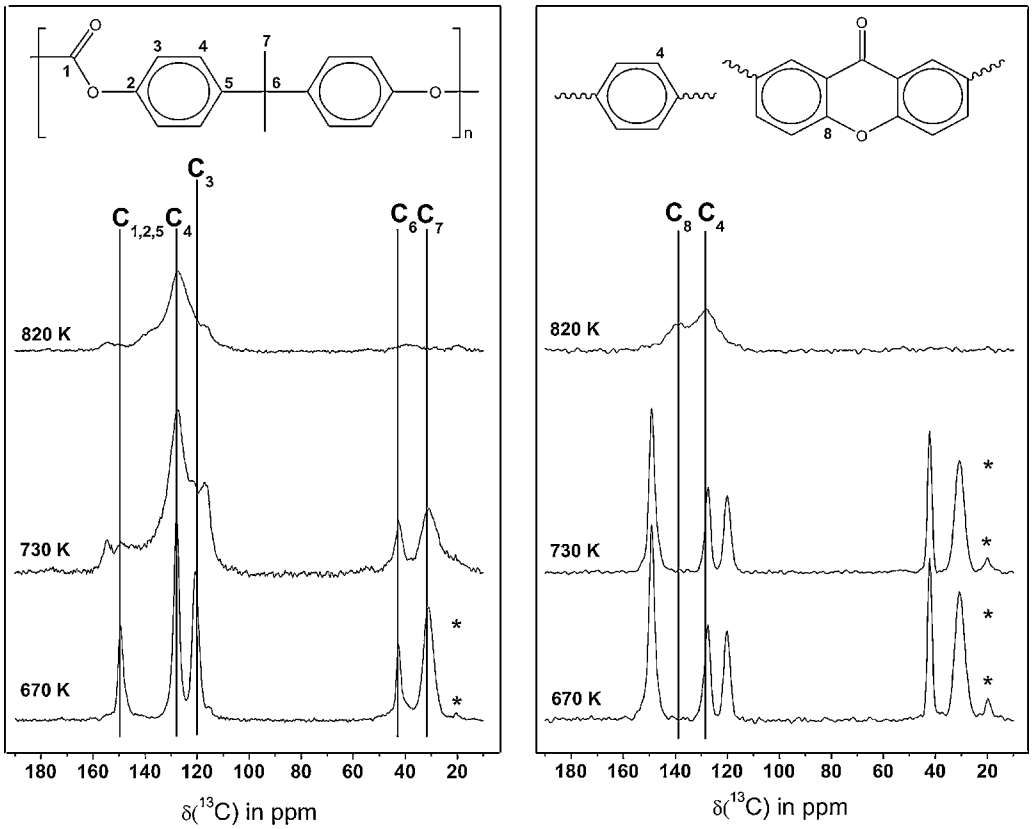

Fig. 5. ^{13}C CPMAS spectra of the solid residues of heated samples at temperatures between 670 and 820 K (N_2, 10 K min^{-1}); on left: PC/ABS + Znb, on right: PC/ABS + BDP + Znb. Asterisks mark MAS spinning sidebands.

The fire behaviour under forced-flaming conditions in the cone calorimeter was discussed in detail for PC/ABS and PC/ABS + BDP in one of our previous papers [6]. All of the heat release rate curves (Fig. 8) show the typical shape for charring polymers, with the peak heat release rate (pHRR) right after the initial increase when the char layer is formed. Further, all investigated PC/ABS materials showed intensive deformation during the cone calorimeter tests, influencing the HRR and pHRR. There is no clear flame-out, but rather a continuous change-over from burning to afterglowing. BDP works as efficient flame retardant in PC/ABS, decreasing both the THR that characterizes the fire load observed in the cone calorimeter and the pHRR that influences the fire growth. BDP in PC/ABS + BDP introduces additional charring (increased residue) or/and improved barrier properties, respectively, in the condensed phase, and flame inhibition (reduction in the THR/ML = total heat release per mass loss) in the gas phase. The flame inhibition depends on the irradiance applied. It increases with increasing irradiation and nearly vanishes upon application of 35 kW m^{-2}. Apart from the pHRR, PC/ABS + Znb showed cone calorimeter results somewhat similar to PC/ABS. The THR and the amount of residue were very similar for 50 and 70 kW m^{-2}, whereas THR is increased and the residue decreased upon application of 35 kW m^{-2}. Considering the fact that the addition of 5 wt.% Znb results in less polymer, the THR of PC/ABS + Znb normalized with the polymer content is worsened and the carbonaceous char yield is decreased. Part of the carbonaceous char is replaced by inorganic residue, accompanied by the release of more carbon as fuel into the flame. This was confirmed by slightly higher THR/ML. In some contrast to the impact on the fire risk THR, the pHRR was decreased. As there was neither a gas-phase activity (no decrease in THR/ML) nor additional charring in the condensed phase (no increase in residue) observed, this behaviour is attributed to an enhanced barrier effect of the inorganic–organic char of PC/ABS + Znb compared to the organic char of PC/ABS. Barrier effects due to the formation of glassy borate coatings are known from the literature [22,23]. The pronounced specific impact of inorganic-carbonaceous barrier on the pHRR without reducing THR is also observed for layered silicate in polymer nanocomposites [24–26].

The total smoke release per mass loss (TSR/ML) indicated that no smoke suppressant effect occurred for PC/ABS + Znb compared to PC/ABS.

Combining Znb and BDP in PC/ABS, the cone calorimeter results for a low external heat flux of 35 kW m^{-2} first of all confirmed the synergistic effect observed in the LOI. The pHRR was decreased without increasing the burning time and the THR decreased compared to PC/ABS + BDP. As the THR/ML of PC/ABS + BDP + Znb for

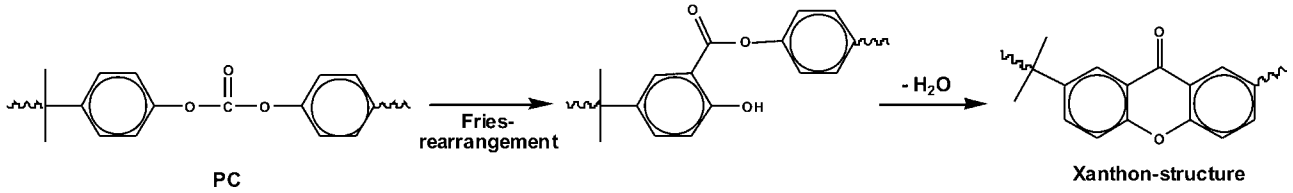

Fig. 6. Xanthon-like structure as secondary product from Fries rearrangements of PC.

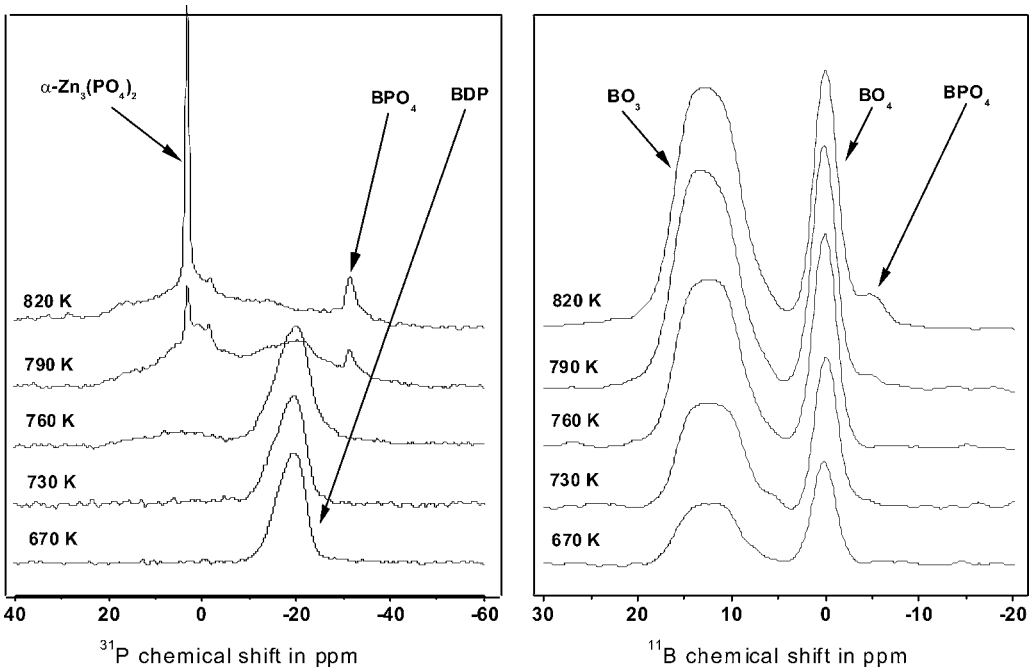

Fig. 7. ^{31}P (left) and ^{11}B MAS NMR measurements (right) for heated PC/ABS + BDP + Znb samples at different temperatures.

35 kW m^{-2} was very similar to the value of the PC/ABS, there is no gas-phase mechanism responsible for these positive effects. The flame retardancy is accompanied by an increased residue, indicating condensed-phase mechanisms. In particular an enhanced barrier effect is concluded, decreasing the pHRR and resulting in extinction before all of the combusted material is consumed.

In Table 3 main cone calorimeter results in dependence on the heat flux are illustrated. In contrast to the increase of residue at 35 kW m^{-2}, for 50 and 70 kW m^{-2} the residue for PC/ABS + BDP + Znb was quite similar to the one from PC/ABS + BDP, even though it contained 4.5 wt.% inert Znb. An increased release of carbon and thus fuel is indicated. The THR was increased for PC/ABS + BDP + Znb compared to PC/ABS + BDP. For 70 kW m^{-2}, the THR for PC/ABS + BDP + Znb was almost as high as for PC/ABS and much higher than for PC/ABS + BDP without Znb. An increased burning time indicated that the barrier was still there, but able only to delay the consumption of combustible material, not to disrupt pyrolysis as was observed for 35 kW m^{-2}. Hence for higher heat fluxes (50 and 70 kW m^{-2}) the fire retardancy of PC/ABS + BDP + Znb was worsened compared to PC/ABS + BDP with respect to THR. Two reasons for this are indicated: (i) the increased release of carbon and (ii) the increase in THR/ML for PC/ABS + BDP + Znb compared to PC/ABS + BDP. The latter is due to a switching off of the flame inhibition effect of BDP when it was combined with Znb. This effect has been reported before for the combustion efficiency of PC/ABS, PC/ABS + BDP and PC/ABS + BDP + Znb using cone calorimeter and pyrolysis combustion flow calorimeter (PCFC) results in the literature [27]. Further, both the reduced carbonaceous charring due to the interaction between PC and BDP and the reduced phosphorus release correspond to the presented pyrolysis investigation, indicating the alternative reaction of BDP and Znb in the condensed phase. Measurements of the phosphorus content of the fire residues suggested that nearly all of the phosphorus stayed in the residue. The switching off of the flame inhibition was accompanied by a reduction in smoke release solely through the improved combustion efficiency.

PC/ABS + BDP + Znb showed the greatest reduction in pHRR: around 30%, 40% and 50% reduction for 35, 50 and 70 kW m^{-2}, respectively (Table 3). The relative effect is equal to the size, assuming both relative effects observed when BDP is added in PC/ABS + BDP and Znb in PC/ABS + Znb, decreasing the pHRR in a serial manner. Somewhat analogous results have been reported for red phosphorus and magnesium hydroxide [28,29], for which the reaction to amorphous metal phosphate reduces the release of phosphorus and yields improved barrier properties of the char.

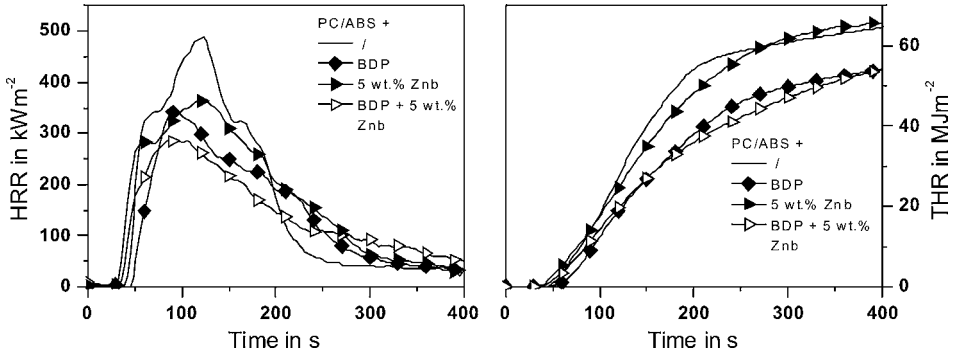

Fig. 8. Heat release rate (HRR) und total heat release (THR) for PC/ABS, PC/ABS + BDP, PC/ABS + Znb and PC/ABS + BDP + Znb, applying an external heat flux of 50 kW m^{-2}.

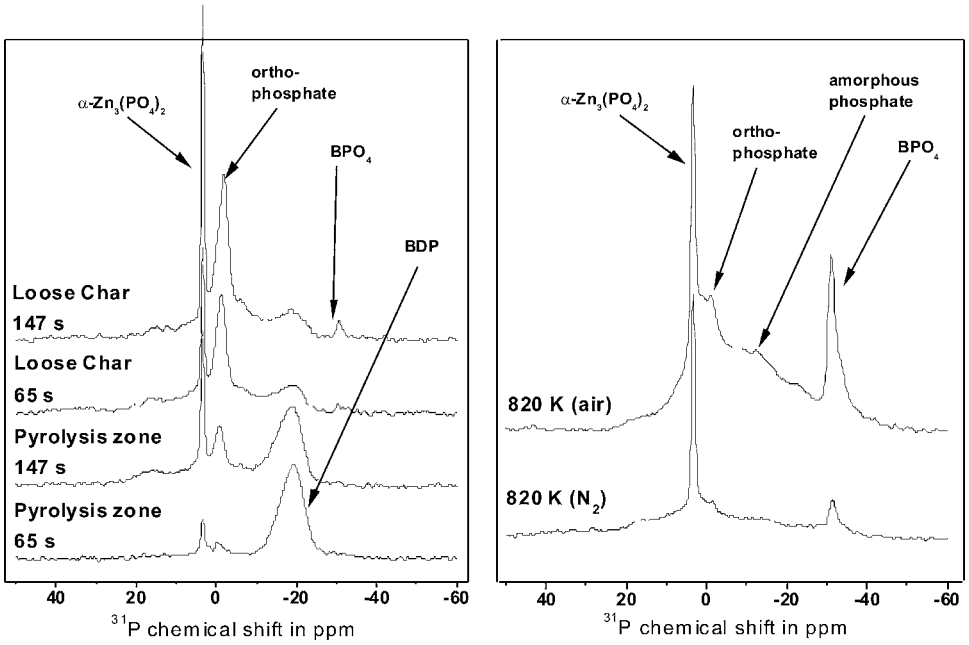

Fig. 9. ^{31}P MAS NMR results for heated PC/ABS + BDP + Znb samples. Left: samples from disrupted cone calorimeter tests, taken after 65 and 147 s, respectively, at top (loose char) and underneath (pyrolysis zone), right: comparison of spectra under air and nitrogen atmosphere.

NMR investigations of cone calorimeter residues were performed to gain insight into the chemical reactions behind the condensed-phase mechanisms that differ for the investigated materials and change with increasing heat flux applied. For this purpose cone calorimeter measurements were run and disrupted by simultaneous extinction and quenching in liquid nitrogen. The samples for the NMR measurements were taken from the black-coloured top, which represents the loose char after combustion, and from the underlying solid layer, which corresponds to the pyrolysis zone. These spectra are shown in the left of Fig. 9. In the pyrolysis zone BDP is the main phosphate component and some α-$Zn_3(PO_4)_2$ is also formed, but no BPO_4. BPO_4 is detected only in the loose char, in which temperatures clearly higher than the pyrolysis temperature of PC were reached. This result and its interpretation are consistent with the thermal analysis presented before. The formation of BPO_4 requires higher temperatures than the formation of α-$Zn_3(PO_4)_2$. However, also reactions with left-over oxygen below the flame may accumulate in the loose residue on the top of the sample. Thus samples were also heated under air to check for any possible influence of present oxygen, in particular on the P:O ratio controlling the formation of the different phosphates. The spectra on the right of Fig. 9 show that α-$Zn_3(PO_4)_2$ and BPO_4 were formed both under thermo-oxidative (air) and under thermal (nitrogen) conditions. In air, though, more BPO_4 is formed and a much higher amount of orthophosphate is built, presumably caused by additional oxygen from the air shifting the P:O ratio towards 1:4. In the pyrolysis zone the ratio of α-$Zn_3(PO_4)_2$ to BPO_4 corresponded to the results of the heated samples under nitrogen atmosphere. Therefore anaerobe decomposition controlling the pyrolysis is confirmed. For the loose char the amount of orthophosphates increased, which indicates an additional thermo-oxidative impact.

Table 3
Fire behaviour of PC/ABS, PC/ABS + BDP, PC/ABS + 5 wt.% Znb and PC/ABS + BDP + 5 wt.% Znb.

PC/ABS + . . .	/	BDP	5 wt.% Znb	BDP + 5 wt.% Znb	Error
Ignition/flammability					
t_{ign}, 35 kW m^{-2} (s)	83	96	75	76	±5
LOI (wt.%)	23.6	28.1	25.5	32.7	±1
UL 94 (1.5 mm)	HB	V-0	HB	V-1	
UL 94 (3 mm)	HB	V-0	HB	V-0	
Flaming combustion (cone calorimeter); irradiation: 35 kW m^{-2}					
THR (MJ m^{-2})	44	46	58	36	±7
pHRR (kW m^{-2})	366	323	288	254	±25
Residue (wt.%)	47	41	35	59	±3
THR/ML (MJ m^{-2} g^{-1})	2.3	2.2	2.5	2.3	±0.1
Burning time (s)	189	228	299	199	±20
TSR/ML (g^{-1})	111	134	94	99	±15
Flaming combustion (cone calorimeter); irradiation: 50 kW m^{-2}					
THR (MJ m^{-2})	60	45	63	51	±7
pHRR (kW m^{-2})	555	357	370	290	±25
Residue (wt.%)	29	35	31	41	±3
THR/ML (MJ m^{-2} g^{-1})	2.4	2.0	2.5	2.3	±0.1
Burning time (s)	170	172	240	246	±20
TSR/ML (g^{-1})	90	161	114	121	±15
Flaming combustion (cone calorimeter); irradiation: 70 kW m^{-2}					
THR (MJ m^{-2})	64	45	62	60	±7
pHRR (kW m^{-2})	616	412	489	332	±25
Residue (wt.%)	25	32	31	31	±3
THR/ML (MJ m^{-2} g^{-1})	2.4	1.8	2.5	2.2	±0.1
Burning time (s)	193	163	205	265	±20
TSR/ML (g^{-1})	122	170	116	134	±15

The added amount of Znb contained enough Zn to consume 90% of the phosphorus added by BDP. The added B can consume up to 64% of the phosphorus. Hence the reaction of BDP with Znb is concluded to compete with the release of phosphorus and with the reaction between BDP and PC decomposition products. The formation of α-$Zn_3(PO_4)_2$ and borophosphates decreases flame inhibition and charring mechanisms based on BDP, as observed for PC/ABS + BDP + Znb in comparison to PC/ABS + BDP at high external heat fluxes.

For LOI and at low external heat flux in the cone calorimeter, PC/ABS + BDP + Znb shows a superior performance, indicating that the deteriorating consumption of BDP and the alternative improved barrier performance are not the only effects occurring. The formed inorganic–organic residue caused an additional flame retarding effect with respect to residue and THR, particularly when such low irradiations are applied. This is somehow surprising, since the common barrier effect reducing the pHRR showed an increasing impact

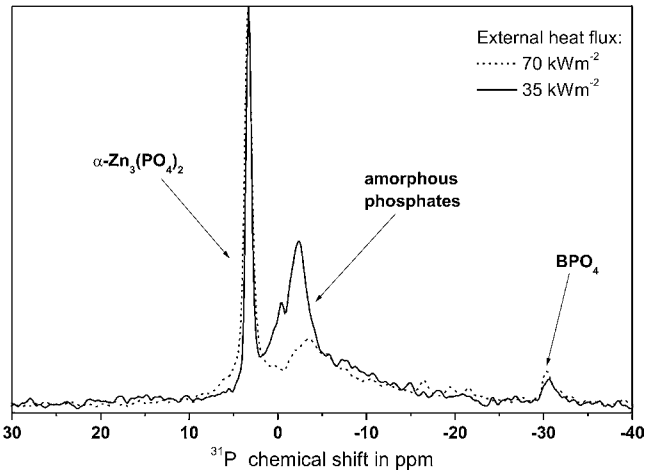

Fig. 10. ^{31}P MAS NMR results of PC/ABS + BDP + Znb fire residues applying different external heat fluxes in the cone calorimeter. Data were normalized to the maximum.

with increasing irradiation and not for decreasing irradiation, as has been reported for other systems in the literature [27,30,31]. In Fig. 10 the NMR results of PC/ABS + BDP + Znb fire residues are shown when irradiations of 35 and 70 kW m^{-2} were applied in the cone calorimeter. For the lower irradiation many more amorphous orthophosphates were built than for 70 kW m^{-2} in comparison to crystalline α-$Zn_3(PO_4)_2$. It is assumed that particularly the amorphous structures, such as those that occur when lower irradiations are applied, cause additional flame retardancy benefits.

4. Conclusion

The addition of 5 wt.% Znb to PC/ABS results in a slightly increased LOI and no significant change in UL 94. Under forced-flaming behaviour a decreased pHRR was obtained, caused by enhanced barrier effects through the inorganic–organic residue in comparison to the carbonaceous char of PC/ABS.

Combining BDP with 5 wt.% Znb in PC/ABS leads to a reaction between both additives. The almost complete conversion of BDP and Znb to alpha-zinc phosphate and borophosphate leaves neither phosphorus to perform flame inhibition in the gas phase nor phosphorus to induce cross-linking in the condensed phase. Instead alpha-zinc phosphate, unspecific orthophosphates and borophosphate act as a barrier to hinder mass and heat transport.

The effectiveness of the combination of BDP and Znb depends on the fire scenario. For an external heat flux of 35 kW m^{-2} and for LOI, which represent the beginning of a fire and the flammability (reaction to small flame), a significant synergism was obtained. The formed barrier, consisting of highly amorphous phosphates, results in better flame retardancy than the gas-phase and condensed-phase mechanisms of BDP in PC/ABS. However, for UL 94 representing an upward flame spread, specimens with a thickness of 3 mm achieved V-0 with a little longer after burning time than PC/ABS + BDP without Znb, and for 1.5 mm the performance was worsened from V-0 to V-1. Also for a fire scenario of a more developed fire, as represented by higher external heat fluxes (50 and 70 kW m^{-2}), BDP combined with Znb fails as an efficient flame retardant since the reduced pHRR is accompanied by antagonistic behaviour in THR. The resulting barrier of zinc-, boro- and orthophosphates is in essential aspects less effective than the mechanisms of BDP in PC/ABS without Znb.

Although Znb is often used as a smoke suppressant, the effect of 5 wt.% Znb in combination with BDP in PC/ABS was not very pronounced. The reduction of the smoke release was obtained because of a higher combustion efficiency when the flame inhibition effect of BDP vanishes. Furthermore, 5 wt.% Znb in PC/ABS without BDP yielded no smoke reduction at all.

The comprehensive study delivers a picture of the flame retardancy mechanisms that are active and control the fire behaviour. It becomes clear that the mechanisms and thus the efficiency of the flame retardants depend on the applied fire scenario or fire tests, respectively. Thus this study provides a foundation for the further development and optimization of tailor-made halogen-free flame retarded PC/ABS.

Acknowledgements

We gratefully acknowledge the support received from the Bayer MaterialScience AG, and thank in particular Dr. V. Taschner, Dr. T. Eckel and Dr. D. Wittmann.

References

[1] S.V. Levchik, E.D. Weil, Polym. Int. 54 (2005) 981–998.
[2] T. Eckel, in: J. Troitzsch (Ed.), Plastic Flammability Handbook, 3rd ed., Hanser Publishers, Munich, 2004, pp. 158–172.
[3] S.V. Levchik, E.D. Weil, J. Fire Sci. 24 (2006) 137–151.
[4] S.V. Levchik, D.A. Bright, G.R. Alessio, S. Dashevsky, J. Vinyl Add. Technol. 6 (2000) 123–128.
[5] S.V. Levchik, D.A. Bright, G.R. Alessio, S. Dashevsky, J. Vinyl Add. Technol. 7 (2001) 98–103.
[6] K.H. Pawlowski, B. Schartel, Polym. Int. 56 (2007) 1404–1414.
[7] J. Green, J. Fire Sci. 14 (1996) 353–366.
[8] J.W. Hastie, J. Res. Natl. Bur. Stand. A: Phys. Chem. 77A (1973) 733–754.
[9] C.P. Fenimore, G.W. Jones, Combust. Flame 8 (1964) 133–137.
[10] M. Bödinger, T. Eckel, D. Wittmann, H. Alberts, German Patent DE 19530200 A1 (1997).
[11] T. Eckel, D. Wittmann, B. Keller, H. Alberts, German Patent DE 19734666 A1 (1999).
[12] E. Wenz, T. Eckel, V. Buchholz, D. Wittmann, B. Thuermer, United States Patent US 2007/0225441 (2007).
[13] A. Seidel, M. Wagner, J. Endtner, W. Ebeneck, T. Eckel, D. Wittmann, European Patent EP 1570002 B1 (2008).
[14] K.H. Pawlowski, B. Schartel, Polym. Degrad. Stabil. 93 (2008) 657–667.
[15] K.K. Shen, S. Kochesfahani, F. Jouffret, Polym. Adv. Technol. 19 (2008) 469–474.
[16] N.L. Thomas, Plast. Rubber Compos. 32 (2003) 413–419.
[17] R. Benrashid, G.L. Nelson, D.J. Ferm, L.W. Chew, J. Fire Sci. 13 (1995) 224–234.
[18] B. Schartel, T.R. Hull, Fire Mater. 31 (2007) 327–354.
[19] C. Jäger, J. Gottwald, H.W. Spiess, R.J. Newport, Phys. Rev. B 50 (1994) 846–852.
[20] G. Montaudo, S. Carroccio, C. Puglisi, J. Anal. Appl. Pyrol. 64 (2002) 229–247.
[21] M. Villa, K.R. Carduner, G. Chiodelli, Solid State Nucl. Magn. Reson. 27 (2005) 50–64.
[22] F. Carpentier, S. Bourbigot, M. Le Bras, R. Delobel, M. Foulon, Polym. Degrad. Stabil. 69 (2000) 83–92.
[23] K.K. Shen, E. Olson, in: C.A. Wilkie, G.L. Nelson (Eds.), Fire and Polymers IV: Materials and Concepts for Hazard Prevention, ACS Symposium Series 922, ACS, Washington, 2005, pp. 224–236.
[24] J.W. Gilman, R.H. Harris, J.R. Shields, T. Kashiwagi, A.B. Morgan, Polym. Adv. Technol. 17 (2006) 263–271.
[25] T. Kashiwagi, M. Mu, K. Winey, B. Cipriano, S.R. Raghavan, S. Pack, M. Rafailovich, Y. Yang, E. Grulke, J. Shields, R. Harris, J. Douglas, Polymer 49 (2008) 4358–4368.
[26] B. Schartel, M. Bartholmai, U. Knoll, Polym. Adv. Technol. 17 (2006) 772–777.
[27] B. Schartel, K.H. Pawlowski, R.E. Lyon, Thermochim. Acta 462 (2007) 1–14.
[28] M.A. Fichera, U. Braun, B. Schartel, H. Sturm, U. Knoll, C. Jäger, J. Anal. Appl. Pyrol. 78 (2007) 378–386.
[29] U. Braun, B. Schartel, Macromol. Chem. Phys. 205 (2004) 2185–2196.
[30] M. Bartholmai, B. Schartel, Polym. Adv. Technol. 15 (2004) 355–364.
[31] B. Schartel, U. Braun, e-Polymers art. no. 13 (2003).